HAL open science

Diurnal Variability in EMIRS Daytime Observations of Water Ice Clouds During Mars Aphelion-Season

Samuel A. Atwood, Michael D. Smith, Khalid Badri, Christopher S. Edwards, Philip R. Christensen, Michael J. Wolff, François Forget, Saadat Anwar, Nathan Smith, M. R. El-Maarry

To cite this version:

Samuel A. Atwood, Michael D. Smith, Khalid Badri, Christopher S. Edwards, Philip R. Christensen, et al.. Diurnal Variability in EMIRS Daytime Observations of Water Ice Clouds During Mars Aphelion-Season. Geophysical Research Letters, 2022, 49, 10.1029/2022GL099654 . insu-03847105

HAL Id: insu-03847105

https://insu.hal.science/insu-03847105

Submitted on 11 Nov 2022

HAL is a multi-disciplinary open access archive for the deposit and dissemination of scientific research documents, whether they are published or not. The documents may come from teaching and research institutions in France or abroad, or from public or private research centers.

L'archive ouverte pluridisciplinaire **HAL**, est destinée au dépôt et à la diffusion de documents scientifiques de niveau recherche, publiés ou non, émanant des établissements d'enseignement et de recherche français ou étrangers, des laboratoires publics ou privés.

Distributed under a Creative Commons Attribution - NonCommercial - ShareAlike 4.0 International License

Check for updates

ADVANCING EARTH AND SPACE SCIENCE

Geophysical Research Letters

RESEARCH LETTER
10.1029/2022GL099654

Special Section:
The First Results from the Emirates Mars Mission (EMM)

Diurnal Variability in EMIRS Daytime Observations of Water Ice Clouds During Mars Aphelion-Season

Samuel A. Atwood[1,2], Michael D. Smith[3], Khalid Badri[4], Christopher S. Edwards[5], Philip R. Christensen[6], Michael J. Wolff[7], François Forget[8], Saadat Anwar[6], Nathan Smith[5], and M. R. El-Maarry[1]

[1]Space and Planetary Science Center, and Department of Earth Sciences, Khalifa University, Abu Dhabi, UAE, [2]Laboratory for Atmospheric and Space Physics, University of Colorado Boulder, Boulder, CO, USA, [3]NASA Goddard Space Flight Center, Greenbelt, MD, USA, [4]Mohammed Bin Rashid Space Center, Dubai, UAE, [5]Department of Astronomy and Planetary Science, Northern Arizona University, Flagstaff, AZ, USA, [6]School of Earth and Space Exploration, Arizona State University, Tempe, AZ, USA, [7]Space Science Institute, Boulder, CO, USA, [8]Laboratoire de Météorologie Dynamique, Paris, France

Key Points:

- Infrared spectra from the Emirates Mars Infrared Spectrometer were used to obtain water ice cloud optical depths throughout the day
- The aphelion cloud belt had a midday minimum with higher optical depths in the morning and afternoon
- Orographic clouds near volcanoes were observed to increase throughout the afternoon

Correspondence to:
S. A. Atwood,
Samuel.Atwood@lasp.colorado.edu

Citation:
Atwood, S. A., Smith, M. D., Badri, K., Edwards, C. S., Christensen, P. R., Wolff, M. J., et al. (2022). Diurnal variability in EMIRS daytime observations of water ice clouds during Mars aphelion-season. *Geophysical Research Letters*, *49*, e2022GL099654. https://doi.org/10.1029/2022GL099654

Received 18 MAY 2022
Accepted 21 JUL 2022

© 2022. The Authors.
This is an open access article under the terms of the Creative Commons Attribution-NonCommercial-NoDerivs License, which permits use and distribution in any medium, provided the original work is properly cited, the use is non-commercial and no modifications or adaptations are made.

Abstract Diurnal analyses of water ice cloud optical depths retrieved from thermal infrared spectra by the Emirates Mars Infrared Spectrometer showed changing cloud abundance throughout the Martian day. Observations began with the start of the Emirates Mars Mission science phase near the beginning of aphelion-season in Mars Year 36 and included the prominent aphelion cloud belt (ACB) and orographic clouds in the vicinity of volcanoes. A midday minimum with higher morning and afternoon optical depths was typical for the ACB, though with considerable spatial variability in this diurnal pattern. Clouds near volcanoes reached a minimum before local noon and tended to increase in abundance throughout the afternoon. Comparisons against the *Laboratoire de Météorologie Dynamique* global circulation model showed analogous spatial patterns in the diurnal signal, which suggested thermal tides and topographic effects to be the predominant drivers of ACB variability, while more localized circulations affected volcano clouds.

Plain Language Summary Observations from the Emirates Mars Infrared Spectrometer onboard the Emirates Mars Mission (EMM) spacecraft were used to measure the abundance of clouds in the Martian atmosphere and investigate how they changed throughout the day. Due to the unique nature of EMM's high orbit, the observations provided by EMIRS cover all times of day and provide more detailed information about how clouds change as compared to many previous missions. In these results we present information about this daytime cloud variability for different regions on Mars. A prominent region of clouds that is commonly observed near the equator during Mars' cold season—known as the aphelion cloud belt—was observed to reach a minimum near midday, with more clouds typically observed in both the morning and afternoon. Distinct differences were found in clouds observed near volcanoes, which tended to reach a minimum before local noon and increase throughout the afternoon. These results add detail to our understanding of cloud behavior and help us to validate computer models of the Martian atmosphere.

1. Introduction

A considerable record of Martian water ice cloud observations from thermal-infrared spectrometers has now been produced from the combined measurements of numerous Mars missions. From these a general climatology has been developed showing water ice cloud to be a prominent component of the Martian atmosphere with substantial seasonal and spatial variability. However, much of this record is derived from sun-synchronous spacecraft that observe at roughly the same local time across their domain. Water ice cloud formation due to condensation of water vapor means that relatively small changes in atmospheric temperatures can lead to considerable changes in cloud abundance. As a result, diurnal temperature changes, thermal tides, water vapor transport pathways from polar regions, and variable orographic effects may all contribute to diurnal variability in cloud abundance beyond the signal captured by local-time-invariant climatologies (Clancy et al., 2017; Määttänen & Montmessin, 2021).

Efforts to characterize this diurnal variability now include a number of instruments and data sets, however, where local time variable observations of water ice cloud exist, spatial, temporal, or seasonal coverage is often limited. The Thermal Emission Spectrometer (TES) onboard Mars Global Surveyor (MGS) provided the first extensive record of thermal infrared spectra at local times of approximately 2 a.m. and 2 p.m., and helped characterize the

19448007, 2022, 15, Downloaded from https://agupubs.onlinelibrary.wiley.com/doi/10.1029/2022GL099654 by Cochrane France, Wiley Online Library on [10/11/2022]. See the Terms and Conditions (https://onlinelibrary.wiley.com/terms-and-conditions) on Wiley Online Library for rules of use; OA articles are governed by the applicable Creative Commons License

spatial, seasonal, and inter-annual variability of Martian water ice clouds (Smith, 2004). Daytime observations by the Mars Odyssey THEMIS instrument shifted in local time due to an orbital change and indicated increasing water ice cloud optical depths as the afternoon progressed from local times of 14:30 to 19:30 (Smith, 2019). Similar findings from Viking IRTM (Tamppari et al., 2003), MGS Mars Orbiter Camera (Benson et al., 2003), and MRO MARCI (M. J. Wolff et al., 2019) observations showed increasing afternoon optical depths. A general midday minimum in water ice cloud abundance in the aphelion cloud belt (ACB) (a prominent cloud type occurring at low latitudes during Mars aphelion season) has been noted in 6 years of local-time-variable thermal-infrared spectra from the Planetary Fourier Spectrometer (PFS) (Giuranna et al., 2021), and in optical and infrared observations from the OMEGA instrument (Szantai et al., 2021)—both onboard the Mars Express spacecraft. Several observational and modeling studies have also indicated orographically induced clouds that occur in the regions of Martian volcanoes increase throughout the day and may reach a maximum in the afternoons (Akabane et al., 2002; Michaels et al., 2006). Additional studies examining water ice cloud differences between day and night (Pankine et al., 2013; Wilson & Guzewich, 2014; Wilson et al., 2007) have suggested generally higher nighttime water ice cloud abundance. Within this record have been indications of more complex behavior in the development of water ice clouds across spatial, diurnal, and seasonal scales—much of which has not been fully resolved. Such gaps in observational coverage limit our understanding of the behavior of water ice cloud development across these dimensions and hinder efforts to develop Mars atmospheric climatologies, validate global circulation models, and resolve observational anomalies (Clancy et al., 2017; Määttänen & Montmessin, 2021).

In this study, we present the first results of observed diurnal variability in retrieved daytime water ice cloud optical depths from the Emirates Mars Infrared Spectrometer (EMIRS; Amiri et al., 2022; Almatroushi et al., 2021; Edwards et al., 2021)—a thermal-infrared spectrometer onboard the Emirates Mars Mission (EMM) spacecraft capable of observing across all local times and a wide range of latitudes and longitudes. EMIRS began science observations in May 2021 near the beginning of Mars aphelion-season, providing a unique opportunity to improve characterizations of daytime diurnal variability during this important water ice cloud season. Additionally, we compare EMIRS observations against modeled water ice cloud abundances from the *Laboratoire de Météorologie Dynamique* (LMD) global circulation model (GCM) and discuss drivers of diurnal variability in both the equatorial ACB and orographic clouds associated with volcanoes.

2. EMIRS Data and Retrieval

The EMIRS instrument is a thermal-infrared spectrometer capable of measuring the temperature and composition of the Martian lower atmosphere and surface from a high-altitude, low-inclination orbit onboard the EMM spacecraft. Due to the unique nature of this orbit EMIRS observations include temporal sampling across all local times and spatial sampling across nearly all latitudes and longitudes, yielding broad coverage across relatively short timescales on the order of 2 weeks. Spectral coverage spans a wavelength range of 6–∼100 μm (1,666–∼100 cm^{-1}) at selectable resolutions of 5 or 10 cm^{-1}, and allows for the retrieval of temperature profiles from the surface to approximately 40 km, along with dust, water ice, and water vapor column optical depths. A pointing mirror for off-nadir observations is used for regular raster scans across the Martian disk at various points in EMM's approximately 20,000–43,000 km elliptical orbit. The projected EMIRS observation pixel is elliptical, with the size of its major axis varying from approximately 100 to 300 km due to both observation height and angle of the observation. This resolution was found to be sufficient for detection of volcano cloud regions that can extend hundreds of km (Clancy et al., 2017), along with larger scale ACB clouds.

The EMIRS retrieval is adapted from the algorithm used for TES (Conrath et al., 2000; Smith, 2004), and is further described in Smith et al. (2022, this issue). Briefly, the retrieval utilizes a constrained linear inversion to fit EMIRS Level 2 calibrated radiance data for the atmospheric temperature profile, followed by retrieval of dust and water ice optical depth, and water vapor column abundance. In addition, the spectral range of EMIRS allows for fitting of both the 12 μm (825 cm^{-1}) water ice feature used in TES retrievals, and the 40 μm (250 cm^{-1}) feature—where typically higher observed radiances and signal to noise ratios were found to be more robust against surface thermophysical effects—as part of this water ice retrieval. All "optical depth" values reported here for water ice cloud are normal-incidence column-integrated full extinction values (including scattering) and have been referenced to 825 cm^{-1}.

19448007, 2022, 15, Downloaded from https://agupubs.onlinelibrary.wiley.com/doi/10.1029/2022GL099654 by Cochrane France, Wiley Online Library on [10/11/2022]. See the Terms and Conditions (https://onlinelibrary.wiley.com/terms-and-conditions) on Wiley Online Library for rules of use; OA articles are governed by the applicable Creative Commons License

Diurnal analyses that investigate changing cloud optical depth throughout the day are limited to regions with valid retrievals across a range of daytime hours. A valid water ice optical depth quantity is dependent on the uncertainty in both the observation and the retrieval. Random noise is generally relatively small but becomes more important at the lower temperatures that occur near dawn and dusk where observed radiance decreases. In addition, sufficient thermal contrast between the atmosphere and surface is required to distinguish the spectral features of atmospheric constituents. Typically, this thermal contrast is lowest near dawn and dusk, which further increases uncertainty in retrieved water ice optical depths near these times and limits the range of local times covered in this analysis. We compute an estimate of this uncertainty in water ice optical depth for each spectrum and retain only those with uncertainties less than 0.05 for the analyses shown here. Additional sources of uncertainty relate to assumed parameters of the retrieval. Uncertainty in the height of observed clouds is estimated through comparison of the standard retrieval, which distributes clouds above an estimated condensation level for each spectrum, against a version where the condensation level was fixed at one scale height—roughly the median value in the standard retrieval. Following M. Wolff et al. (2006) we use a fixed cloud particle effective radius of 2.0 μm for all retrievals shown here, along with sensitivity testing using effective radius values of 1.0 and 4.0 μm (e.g., Clancy et al., 2003). Sensitivity testing of seasonally averaged optical depths to changes in these assumed parameters yielded differences of less than 0.03 for 95% of the spatially averaged bins shown in the following analysis. Crucially, the sensitivity for both parameters primarily affected the magnitude of the optical depths, while the diurnal and spatial trends remained similar for the various parameter options. Total uncertainty due to all sources discussed here could therefore be estimated at less than 0.08 on a seasonally averaged basis, though these values were higher near dawn and dusk and considerably lower throughout much of the rest of the day. Further sources of uncertainty in observation and parameter selection are discussed in Smith et al. (2022, this issue).

Finally, prior to analysis EMIRS retrievals are filtered to remove spectra with emission angles greater than 70° or surface temperatures less than 190 K to ensure sufficient thermal contrast. Data which passed these quality control checks yielded considerable coverage for all longitudes in daytime hours (nominally 06:00 to 18:00 LTST) across latitudes between roughly 30°S and 45°N for much of the aphelion season. Nighttime retrievals passing these criteria were more limited spatially and temporally. In addition, surface thermophysical effects at the colder surface temperatures typical of nighttime observations necessitate improved representations of these processes in the algorithm to reliably produce valid retrievals. Work to retrieve aerosol optical depths at night is ongoing but is not included here for the bulk of nighttime observations. As a result, here we report analyses of daytime aphelion-season water ice clouds as seasonal averages of the nominal ACB season between L_s = 40°–140°. Actual observational coverage began with the start of EMIRS science observations at L_s = 49° during Mars Year 36, and included all data through L_s = 140°. However, this includes a period of missing data between roughly L_s = 103°–120° due to solar conjunction and a spacecraft safe mode event. Seasonal variability is briefly discussed with data from additional periods through L_s = 180° and includes observations of the end of the ACB.

3. Results

The spatial distribution of EMIRS aphelion-season averaged water ice cloud optical depths is shown for six local times between 07:00 and 17:00 in Figure 1. Existing climatologies and observational data sets typically report the ACB between roughly 10°S and 30°N (shown as black dashed lines in the following figures) (Clancy et al., 2017; Määttänen & Montmessin, 2021). EMIRS observations showed clouds within these latitudinal extents during midday and early afternoon—near the observation time of many of the sun-synchronous instruments. However, in the early morning before roughly 09:00 there was some indication of an extension of the ACB further north of these typical bounds, particularly in the rough terrain regions near Alba Patera. This latitudinal extension of the ACB has been discussed previously as a potential feature of nighttime and morning clouds, and may be more common later in the aphelion-season (Guha et al., 2021; Heavens et al., 2010; Pankine et al., 2013; M. J. Wolff et al., 2019). Longitudinal variability was also evident, with higher optical depths over the Tharsis and Elysium regions, and lower values east of the prime meridian. These observations were consistent with previous reports of typical ACB characteristics (Clancy et al., 2017; Giuranna et al., 2021; Smith, 2004, 2009; M. J. Wolff et al., 2019).

Throughout much of the ACB the lowest optical depths were observed near midday, with higher values often occurring in both the morning and afternoon. Values during the midday minimum ranged from 0.2 to 0.3 over

19448007, 2022, 15, Downloaded from https://agupubs.onlinelibrary.wiley.com/doi/10.1029/2022GL099654 by Cochrane France, Wiley Online Library on [10/11/2022]. See the Terms and Conditions (https://onlinelibrary.wiley.com/terms-and-conditions) on Wiley Online Library for rules of use; OA articles are governed by the applicable Creative Commons License

10.1029/2022GL099654

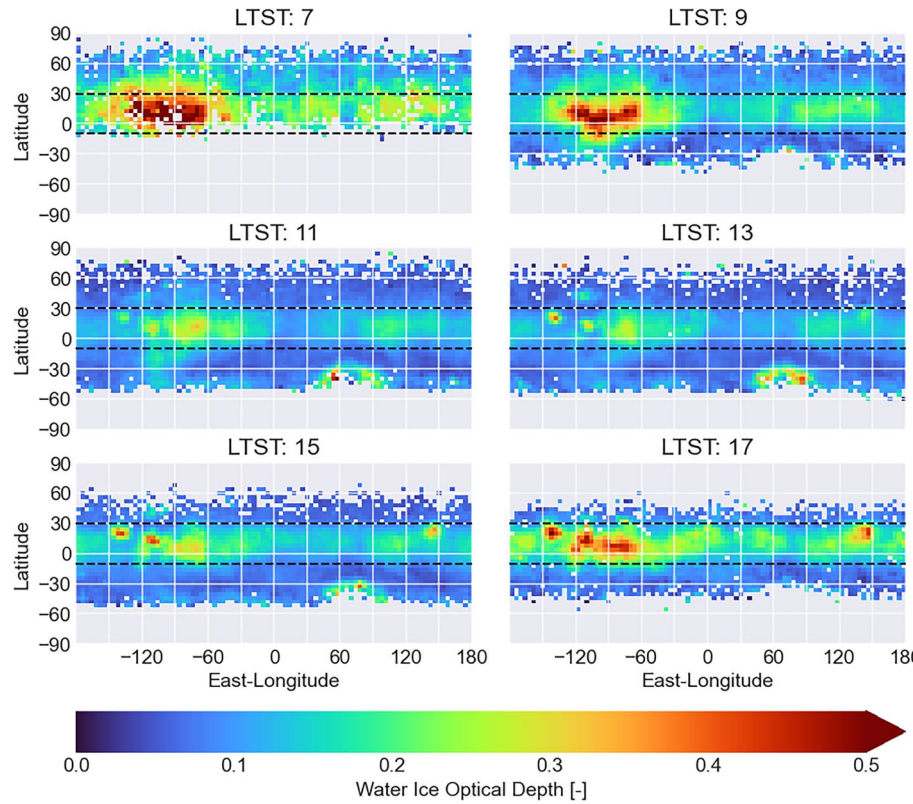

Figure 1. Emirates Mars Infrared Spectrometer (EMIRS) retrieved water ice cloud optical depths averaged for the aphelion-season at six local true solar times. Each 2-hr time period includes all valid data between $L_s = 40°–140°$ and ±1-hr from the LTST time shown with 4° × 4° latitude-longitude bins. Bin smoothing by 2-D Gaussian kernel convolution and nominal aphelion cloud belt (ACB) extents are shown as dashed black lines for all figures.

Tharsis and Elysium, to less than 0.1 in some areas where optical depths were similar to regions outside the ACB. Optical depths exceeded 0.5 in the early morning over Tharsis and reached 0.4–0.5 over volcanoes in the late afternoon. During these near-dawn/dusk time periods the ACB was nearly continuous across all longitudes, with most optical depths exceeding 0.2. Individual retrievals had optical depths up to ∼1, though these were often for early-morning/late-afternoon observations where uncertainties were also high.

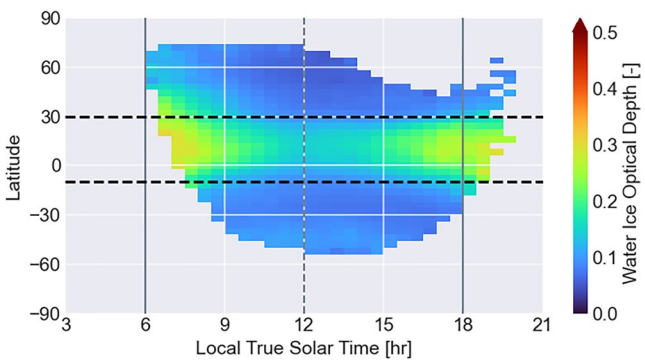

Figure 2. Zonally averaged Emirates Mars Infrared Spectrometer (EMIRS) aphelion-season water ice optical depths for all local times included in this study. Midday and nominal daytime extents for dawn and dusk are shown as gray lines to emphasize some optical depth retrievals extending into the early evening.

Zonally averaged optical depths for the range of observed local times (Figure 2) showed the same general trend as the spatial analysis. A diurnal minimum with optical depths around 0.15 occurred just after local noon within the ACB, while values as high as 0.3 occurred just after dawn and dusk. Values outside of the ACB were generally below 0.1 after midday. However, the impact of the early morning extension of the ACB is evident up to at least 60°N where morning optical depths exceeded the midday values. Also of note were a limited set of retrievals that passed quality checks from local times after 18:00 where thermal contrast was still high enough for a valid retrieval. Water ice cloud optical depths in these spectra showed evidence of continued increases somewhat past dusk with no evidence of a local maximum having been reached. However, spatial differences in the timing of the seasonal-average diurnal minimum varied between 09:00 and 15:00 (not shown, a similar effect is investigated in the parameterization in the next section), complicating this somewhat simple notion of a consistent midday minimum to some extent.

Deviations from this general diurnal pattern in ACB water ice cloud abundance were particularly evident in the vicinity of volcanoes where orographic

19448007, 2022, 15, Downloaded from https://agupubs.onlinelibrary.wiley.com/doi/10.1029/2022GL099654 by Cochrane France, Wiley Online Library on [10/11/2022]. See the Terms and Conditions (https://onlinelibrary.wiley.com/terms-and-conditions) on Wiley Online Library for rules of use; OA articles are governed by the applicable Creative Commons License

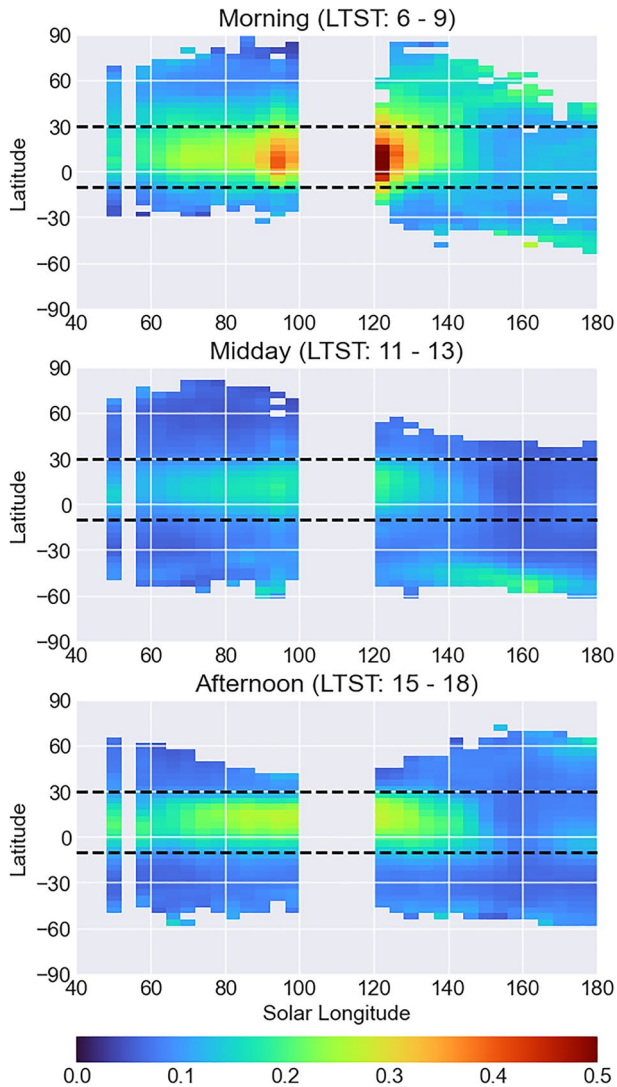

Figure 3. Seasonal progression of zonally averaged Emirates Mars Infrared Spectrometer (EMIRS) water ice optical depths for morning, midday, and afternoon local time periods. While the Emirates Mars Mission (EMM) orbit led to varying diurnal observational coverage by latitude, the aphelion cloud belt (ACB) was well covered across local times throughout the aphelion-season.

clouds form due to upslope winds and lee waves propagating off the high elevation peaks (Benson et al., 2003; Michaels et al., 2006). In the early morning these clouds were often absent or not detectable above the more spatially extensive ACB clouds (Figure 1). As the morning progressed, ACB optical depths decreased and small regions of increasing cloud development were detectable by midday in the regions near Olympus Mons, Tharsis Montes, and Elysium Mons. These orographic cloud regions continued to increase throughout the afternoon and showed no indication of a maximum having been reached by dusk where coverage ends in this analysis. Some indication of similar behavior near Alba Patera was also evident, but with more limited observational coverage making the signal less evident.

Seasonal changes to water ice optical depths were most evident in the magnitude of the cloud abundance, though changes to the spatial distribution of clouds were also observed. The seasonal progression of zonally averaged optical depths is shown for morning, midday, and afternoon local time periods in Figure 3. A similar diurnal signal and midday minimum was evident throughout the season, with a tendency for higher values in the morning as compared to the afternoon. The seasonal peak in optical depth, which typically occurs around $L_s = 105°$, likely occurred during the period of missing data. Nevertheless, the observed maximum near $L_s = 120°$ saw morning and midday optical depths reach values of approximately 0.5 and 0.2, respectively. Seasonal differences in the spatial distribution of water ice cloud were primarily observed in the post-conjunction period after $L_s = 120°$, during which the early morning latitudinal extension to the north of the nominal ACB latitude band was most evident. This behavior was also observed by the Emirates Exploration Imager (EXI) instrument onboard EMM (Jones et al., 2021), and is discussed further by Wolff et al. (2022, this issue). By the nominal end of the ACB at $L_s = 140°$ optical depths showed decreases at all times of day. Interestingly, a regional dust storm that occurred in the mid-southern latitudes from roughly $L_s = 153°–160°$ (discussed further in Smith et al., 2022, this issue) was associated with decreased water ice optical depths at ACB latitudes for all observed times of day. Zonally averaged optical depths at 10°N dropped to their lowest values of the study to roughly 0.05 at midday and as low as 0.1 nearer to dawn and dusk, before recovering after the dust storm had subsided. At the same time, while observational coverage was limited, at northern mid-latitudes higher optical depths around 0.2 persisted in northern fall, perhaps as late as $L_s = 180°$ where coverage in this analysis ended.

3.1. Diurnal Parameterization

Further investigation of the spatial differences in diurnal behavior was conducted using a simple parameterization of the difference in average optical depth between morning, midday, and afternoon time periods. As full diurnal coverage across all daytime hours was not available across all spatial locations, regions used for this parameterization were first filtered for those with sufficient observations for a valid comparison between time periods. First, hourly means for each grid box were computed to ensure more limited sampling closer to dawn and dusk did not skew averaging. From these, mean optical depths were calculated for the morning (local true solar times between 06:00–09:00), midday (11:00–13:00), and afternoon (15:00–18:00). Local time bins with at least three valid retrievals were considered sufficient for averaging purposes and retained in the analysis, leaving approximately 60,000 retrievals used for this parameterization. The difference in optical depths between these periods are shown in Figure 4.

The parameterization shows some of the complexity in the spatial distribution of the diurnal behavior noted in the previous section. Regions with greater morning cloud abundance as compared to the afternoon (blue colors,

19448007, 2022, 15, Downloaded from https://agupubs.onlinelibrary.wiley.com/doi/10.1029/2022GL099654 by Cochrane France, Wiley Online Library on [10/11/2022]. See the Terms and Conditions (https://onlinelibrary.wiley.com/terms-and-conditions) on Wiley Online Library for rules of use; OA articles are governed by the applicable Creative Commons License

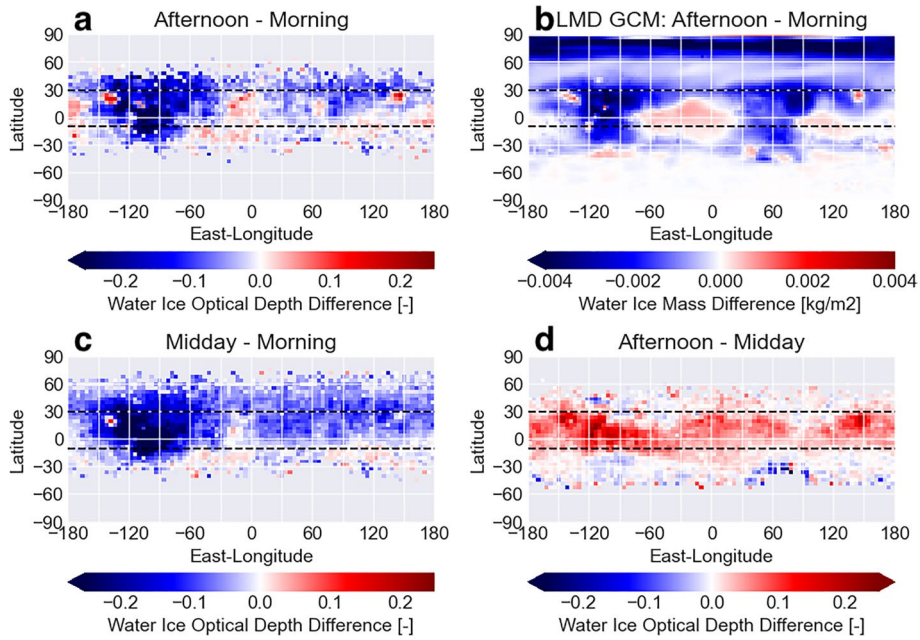

Figure 4. Diurnal parameterization of cloud abundance for the difference between afternoon and morning aphelion-season mean values for (a) Emirates Mars Infrared Spectrometers (EMIRS) observed optical depth and (b) *Laboratoire de Météorologie Dynamique* (LMD) global circulation model (GCM) water ice mass, indicating qualitatively similar spatial patterns in the diurnal signal. Similar parameterizations are shown for differences in EMIRS optical depths between (c) midday and morning, and (d) afternoon and midday. Blue (red) colors indicate decreasing (increasing) optical depths with time.

Figure 4a) were particularly evident over Tharsis—where widespread early morning clouds had been noted and morning optical depths exceeded afternoon values by more than 0.2 in some areas. Conversely, the more localized orographic clouds near volcanoes—which had higher afternoon optical depths (red colors)—were noteworthy for their high contrast against the more widespread ACB clouds in the surrounding regions. Further detail was evident in the parameterizations of morning and afternoon against midday. In the afternoon (Figure 4d) the largest changes in optical depth tended to be confined to regions within the typical ACB latitude band. Changing optical depths in the morning, however, extended further to the north (Figure 4c)—reinforcing the notion of a possible nighttime or early-morning latitudinal extension of the ACB beyond 30°N.

A similar parameterization of the differences in water ice mass between morning and afternoon was generated for LMD GCM output using roughly the same set of seasonal time periods and local time ranges as the EMIRS observations (Figure 4b)—allowing for a qualitative comparison between the observations and model output. Interestingly, substantial qualitative agreement in the spatial distribution for both the ACB and orographic volcano clouds was apparent. Model simulations have attributed much of these large-scale spatial and diurnal patterns in ACB clouds to thermal tides and topographic effects (Hinson & Wilson, 2004; Szantai et al., 2021; Wilson et al., 2007). These are contrasted against the more localized circulations associated with the high elevation topography that drive cloud development near volcanoes (Michaels et al., 2006; Wilson et al., 2007). In both cases the similarity between the parameterizations served as both a validation of the model results and a potential explanation of the drivers of observed diurnal variability.

4. Conclusions and Summary

Water ice optical depth retrievals from EMIRS constitute a new and unique Martian atmospheric data set due in large part to the observational capabilities of the EMM spacecraft. Observational coverage across all local times allowed for an in-depth diurnal analysis of daytime cloud abundance during Mars aphelion-season. Mean water ice cloud optical depths were calculated for all longitudes and latitudes between roughly 30°S and 45°N for the nominal aphelion-season of L_s = 40°–140° during Mars Year 36. The prominent low-latitude ACB was well covered

19448007, 2022, 15, Downloaded from https://agupubs.onlinelibrary.wiley.com/doi/10.1029/2022GL099654 by Cochrane France, Wiley Online Library on [10/11/2022]. See the Terms and Conditions (https://onlinelibrary.wiley.com/terms-and-conditions) on Wiley Online Library for rules of use; OA articles are governed by the applicable Creative Commons License

in this data set with extensive spatial and temporal sampling beyond what previous missions were able to achieve over a single season. The lowest daytime water ice optical depths typically occurred near midday for these clouds, with higher values occurring in both the mornings and afternoons. Comparison of morning and afternoon optical depths indicated generally higher values in the morning, though with considerable spatial variability. Analogous spatial patterns in the diurnal variability found in model results were driven by large-scale thermal tides and topographic effects in the case of the ACB. In the vicinity of volcanoes, where more localized circulations were dominant, orographic water ice clouds formed by midday and increased in opacity throughout the afternoon in both the EMIRS observations and model output. These results were generally consistent with expectations based on previous observational datasets and model findings (Clancy et al., 2017; Määttänen & Montmessin, 2021). However, the observational coverage provided by EMIRS allowed for more detailed analysis of the diurnal signal in water ice cloud development—especially in the morning hours when fewer observations have historically taken place. Climatologies largely based on mid-afternoon observations from sun-synchronous spacecraft typically report the ACB constrained to latitudes between roughly 10°S and 30°N. However, some nighttime water ice cloud studies and model results have found wider latitudinal extents to this belt (Guha et al., 2021; Heavens et al., 2010; Pankine et al., 2013; M. J. Wolff et al., 2019). Consistent with these expectations, EMIRS found an early morning latitudinal extension of water ice clouds further north of 30°N, particularly in the region of Tharsis and during northern summer after roughly $L_s = 120°$. This extension tended to decrease back to the typically reported bounds by late-morning or midday—consistent with the findings of the mid-afternoon observations (e.g., Smith, 2004). Previous studies have also indicated nighttime clouds in the ACB are likely to be more abundant than during the day (Pankine et al., 2013; Wilson & Guzewich, 2014; Wilson et al., 2007). This is consistent with the general diurnal pattern described in this work, which found the highest daytime values near dawn and dusk. Future work using EMIRS spectra will therefore focus on nighttime retrievals and extending the diurnal analysis to a full Martian sol.

Data Availability Statement

Data from the Emirates Mars Mission (EMM) are freely and publicly available on the EMM Science Data Center (SDC, http://sdc.emiratesmarsmission.ae). This location is designated as the primary repository for all data products produced by the EMM team and is designated as long-term repository as required by the UAE Space Agency. The data available (http://sdc.emiratesmarsmission.ae/data) include ancillary spacecraft data, instrument telemetry, Level 1 (raw instrument data) to Level 3 (derived science products), quicklook products, and data users guides (https://sdc.emiratesmarsmission.ae/documentation) to assist in the analysis of the data. Following the creation of a free login, all EMM data are searchable via parameters such as product file name, solar longitude, acquisition time, sub-spacecraft latitude & longitude, instrument, data product level, etc.

Data products can be browsed within the SDC via a standardized file system structure that follows the convention:

/emm/data/<Instrument>/<DataLevel>/<Mode>/<Year>/<Month>

Data product filenames follow a standard convention:

emm_<Instrument>_<DataLevel><StartTimeUTC>_<OrbitNumber>_<Mode>_<Description>_<KernelLevel>_<Version>.<FileType).

EMIRS data and users guides are available at: https://sdc.emiratesmarsmission.ae/data/emirs.

Acknowledgments
SAA is supported by the grant (8474000332-KU-CU-LASP Space Sci.)

References

Akabane, T., Nakakushi, T., Iwasaki, K., & Larson, S. M. (2002). Diurnal variation of Martian water-ice clouds in Tharsis region of the low latitude cloud belt: Observations in 1995–1999 apparitions. *Astronomy & Astrophysics*, *384*(2), 678–688. https://doi.org/10.1051/0004-6361:20020030

Almatroushi, H., AlMazmi, H., AlMheiri, N., AlShamsi, M., AlTunaiji, E., Badri, K., et al. (2021). Emirates Mars Mission characterization of Mars atmosphere dynamics and processes. *Space Science Reviews*, *217*(8), 89. https://doi.org/10.1007/s11214-021-00851-6

Amiri, H. E. S., Brain, D., Sharaf, O., Withnell, P., McGrath, M., Alloghani, M., et al. (2022). The Emirates Mars Mission. *Space Science Reviews*, *218*(1), 4. https://doi.org/10.1007/s11214-021-00868-x

Benson, J. L., Bonev, B. P., James, P. B., Shan, K. J., Cantor, B. A., & Caplinger, M. A. (2003). The seasonal behavior of water ice clouds in the Tharsis and Valles Marineris regions of Mars: Mars orbiter camera observations. *Icarus*, *165*(1), 34–52. https://doi.org/10.1016/S0019-1035(03)00175-1

Clancy, R. T., Montmessin, F., Benson, J. L., Daerden, F., Colaprete, A., & Wolff, M. J. (2017). Mars Clouds. In *The atmosphere and climate of Mars*. Cambridge University Press.

19448007, 2022, 15, Downloaded from https://agupubs.onlinelibrary.wiley.com/doi/10.1029/2022GL099654 by Cochrane France, Wiley Online Library on [10/11/2022]. See the Terms and Conditions (https://onlinelibrary.wiley.com/terms-and-conditions) on Wiley Online Library for rules of use; OA articles are governed by the applicable Creative Commons License

Clancy, R. T., Wolff, M. J., & Christensen, P. R. (2003). Mars aerosol studies with the MGS TES emission phase function observations: Optical depths, particle sizes, and ice cloud types versus latitude and solar longitude. *Journal of Geophysical Research*, *108*(E9), 5098. https://doi.org/10.1029/2003JE002058

Conrath, B. J., Pearl, J. C., Smith, M. D., Maguire, W. C., Christensen, P. R., Dason, S., & Kaelberer, M. S. (2000). Mars Global Surveyor Thermal Emission Spectrometer (TES) observations: Atmospheric temperatures during aerobraking and science phasing. *Journal of Geophysical Research*, *105*(E4), 9509–9519. https://doi.org/10.1029/1999JE001095

Edwards, C. S., Christensen, P. R., Mehall, G. L., Anwar, S., Tunaiji, E. A., Badri, K., et al. (2021). The Emirates Mars Mission (EMM) Emirates Mars InfraRed spectrometer (EMIRS) instrument. *Space Science Reviews*, *217*(7), 77. https://doi.org/10.1007/s11214-021-00848-1

Giuranna, M., Wolkenberg, P., Grassi, D., Aronica, A., Aoki, S., Scaccabarozzi, D., et al. (2021). The current weather and climate of Mars: 12 years of atmospheric monitoring by the Planetary Fourier spectrometer on Mars Express. *Icarus*, *353*, 113406. https://doi.org/10.1016/j.icarus.2019.113406

Guha, B. K., Panda, J., & Wu, Z. (2021). Observation of aphelion cloud belt over Martian tropics, its evolution, and associated dust distribution from MCS data. *Advances in Space Research*, *67*(4), 1392–1411. https://doi.org/10.1016/j.asr.2020.11.010

Heavens, N. G., Benson, J. L., Kass, D. M., Kleinböhl, A., Abdou, W. A., McCleese, D. J., et al. (2010). Water ice clouds over the Martian tropics during northern summer. *Geophysical Research Letters*, *37*(18). https://doi.org/10.1029/2010GL044610

Hinson, D. P., & Wilson, R. J. (2004). Temperature inversions, thermal tides, and water ice clouds in the Martian tropics. *Journal of Geophysical Research*, *109*(E1), E01002. https://doi.org/10.1029/2003JE002129

Jones, A. R., Wolff, M., Alshamsi, M., Osterloo, M., Bay, P., Brennan, N., et al. (2021). The Emirates exploration Imager (EXI) instrument on the Emirates Mars Mission (EMM) hope Mission. *Space Science Reviews*, *217*(8), 81. https://doi.org/10.1007/s11214-021-00852-5

Määttänen, A., & Montmessin, F. (2021). Clouds in the Martian atmosphere. https://doi.org/10.1093/acrefore/9780190647926.013.114

Michaels, T. I., Colaprete, A., & Rafkin, S. C. R. (2006). Significant vertical water transport by mountain-induced circulations on Mars. *Geophysical Research Letters*, *33*(16), L16201. https://doi.org/10.1029/2006GL026562

Pankine, A. A., Tamppari, L. K., Bandfield, J. L., McConnochie, T. H., & Smith, M. D. (2013). Retrievals of Martian atmospheric opacities from MGS TES nighttime data. *Icarus*, *226*(1), 708–722. https://doi.org/10.1016/j.icarus.2013.06.024

Smith, M. D. (2004). Interannual variability in TES atmospheric observations of Mars during 1999–2003. *Icarus*, *167*(1), 148–165. https://doi.org/10.1016/j.icarus.2003.09.010

Smith, M. D. (2009). THEMIS observations of Mars aerosol optical depth from 2002–2008. *Icarus*, *202*(2), 444–452. https://doi.org/10.1016/j.icarus.2009.03.027

Smith, M. D. (2019). Local time variation of water ice clouds on Mars as observed by THEMIS. *Icarus*, *333*, 273–282. https://doi.org/10.1016/j.icarus.2019.06.009

Smith, M. D., Badri, K., Atwood, S. A., Edwards, C. S., Christensen, P. R., Wolff, M. J., et al. (2022). EMIRS observations of the aphelion-season Mars atmosphere. *Geophysical Research Letters*. in press. https://doi.org/10.1029/2022gl099636

Szantai, A., Audouard, J., Forget, F., Olsen, K. S., Gondet, B., Millour, E., et al. (2021). Martian cloud climatology and life cycle extracted from Mars Express OMEGA spectral images. *Icarus*, *353*, 114101. https://doi.org/10.1016/j.icarus.2020.114101

Tamppari, L. K., Zurek, R. W., & Paige, D. A. (2003). Viking-era diurnal water-ice clouds. *Journal of Geophysical Research*, *108*(E7), 5073. https://doi.org/10.1029/2002JE001911

Wilson, R. J., & Guzewich, S. D. (2014). Influence of water ice clouds on nighttime tropical temperature structure as seen by the Mars Climate Sounder. *Geophysical Research Letters*, *41*(10), 3375–3381. https://doi.org/10.1002/2014GL060086

Wilson, R. J., Neumann, G. A., & Smith, M. D. (2007). Diurnal variation and radiative influence of Martian water ice clouds. *Geophysical Research Letters*, *34*(2), L02710. https://doi.org/10.1029/2006GL027976

Wolff, M. J., Clancy, R. T., Kahre, M. A., Haberle, R. M., Forget, F., Cantor, B. A., & Malin, M. C. (2019). Mapping water ice clouds on Mars with MRO/MARCI. *Icarus*, *332*, 24–49. https://doi.org/10.1016/j.icarus.2019.05.041

Wolff, M. J., Fernando, A., Smith, M. D., Forget, F., Millour, E., Atwood, S. A., et al. (2022). Diurnal variations in the aphelion cloud belt as observed by the Emirates Exploration Imager (EXI). *Geophysical Research Letters*. in press.

Wolff, M. J., Smith, M. D., Clancy, R. T., Spanovich, N., Whitney, B. A., Lemmon, M. T., et al. (2006). Constraints on dust aerosols from the Mars Exploration Rovers using MGS overflights and Mini-TES. *Journal of Geophysical Research*, *111*(E12), E12S17 https://doi.org/10.1029/2006JE002786

19448007, 2022, 15, Downloaded from https://agupubs.onlinelibrary.wiley.com/doi/10.1029/2022GL099654 by Cochrane France, Wiley Online Library on [10/11/2022]. See the Terms and Conditions (https://onlinelibrary.wiley.com/terms-and-conditions) on Wiley Online Library for rules of use; OA articles are governed by the applicable Creative Commons License